J|A|C|S
COMMUNICATIONS

Published on Web 05/02/2006

# Scanning Tunneling Spectroscopy in an Ionic Liquid

Tim Albrecht,[†] Kasper Moth-Poulsen,[‡] Jørn B. Christensen,[‡] Johan Hjelm,[§] Thomas Bjørnholm,*[,‡] and Jens Ulstrup*[,†]

*Department of Chemistry, Nano•DTU, Technical University of Denmark, Building 207, 2800 Kongens Lyngby, Denmark, H.C. Ørsted Institute, NanoScience Center, University of Copenhagen, 2100 Copenhagen, Denmark, and Department for Fuel Cells and Solid State Chemistry, Risø National Laboratory, Frederiksborgvej 399, 4000 Roskilde, Denmark*

Received April 4, 2006; E-mail: ju@kemi.dtu.dk; tb@nano.ku.dk

In this communication, we report, for the first time, the application of an ionic liquid, 1-butyl-3-methylimidazoliumhexafluorophosphate (BMI), as an electrochemical gate medium for tunneling spectroscopy at the single-molecule scale. In a proof-of-principle experiment, we use the Os(II)/Os(III) redox transition of a heteroleptic redox-active Os bisterpyridine complex (Ossac) to achieve tunneling current modulation at room temperature.[1−8] One terpyridine ligand is functionalized with a 6-acetylthiohexyloxy linker to achieve efficient binding to Au(111) electrode surfaces. The surface redox potential of Ossac is determined by monolayer cyclic voltammetry (CV) (Figure 1). The black CV was measured in aqueous 0.1 M $HClO_4$. The surface redox potential was determined to be $E^0_{surf} = +0.68$ V versus saturated calomel electrode (SCE), in good agreement with solution redox potentials of closely related Os complexes.[3,4,9]

The small peak separation even at low scan rates is due to ion pairing with $ClO_4^-$, which also explains the slight peak asymmetry. The red CV has been measured in BMI. The CV signals are broader, with a larger peak separation which remains constant at low scan rates. The average peak potential serves as a common reference in Figure 1.

Irrespective of thermodynamic details of the electron transfer (ET) process, the key point is that the redox level can be used for tunneling current modulation, also in an ionic liquid. To probe this effect, we employed an electrochemical Scanning Tunneling Microscope (STM). In contrast to STM in air or vacuum, tip and substrate potentials are controlled independently with respect to a common reference electrode. This offers two spectroscopic tools: $I_t(V_{bias})$ spectroscopy at constant substrate potential $E_s$ and $I_t(E_s)$ spectroscopy at constant tip/substrate bias $V_{bias}$ ($V_{bias} = E_t - E_s$).[10]

The latter is exemplified in Figure 2, $V_{bias} = +0.7$ V (cf. Methods). The tunneling current increases from the initial value $I_{set}{}^0 = 0.05$ nA at $E_{s,i} = -0.85$ V versus the anodic peak position in CV, $E_p{}^{an}$, to 2.3 nA, corresponding to an on/off ratio of ∼50. The enhancement factor depends on the number of molecules that contribute to the tunneling process. Due to the strong distance dependence of the tunneling current, this number is small, ∼1−10. The enhancement also depends on the charge transport mechanism. We have previously shown that electron hopping is likely to dominate at small $V_{bias}$ ($kT < eV_{bias} <$ reorganization free energy $\lambda$).[3,4]

The feature in Figure 2 resembles transistor function, but the independent control of tip and substrate potential can be used to induce rectifying behavior, as well.[11] For example, if the substrate potential $E_s$ is set to a potential "left" of the peak in Figure 2, $E_{s,0}$, and the tip potential $E_t$ swept symmetrically around $E_{s,0}$, a strong current increase is expected for $V_{bias} > 0$ V (Figure 3). Only in this bias direction the redox level(s) associated with $E^0_{surf}$ will enter

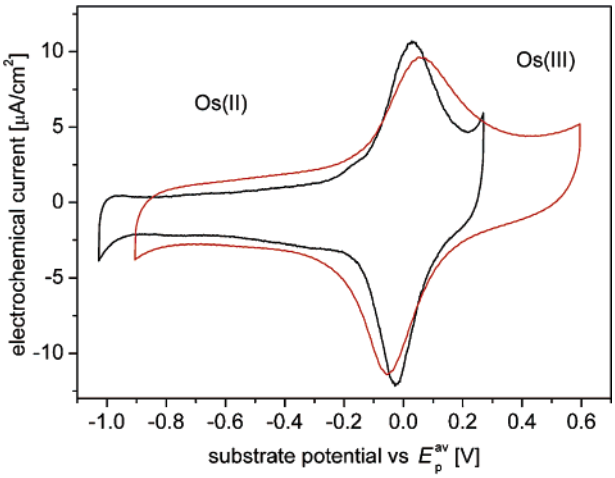


***Figure 1.*** CV data of Ossac on Au(111) in aqueous 0.1 M $HClO_4$ (black) and BMI (red); scan rate = 0.1 V/s.

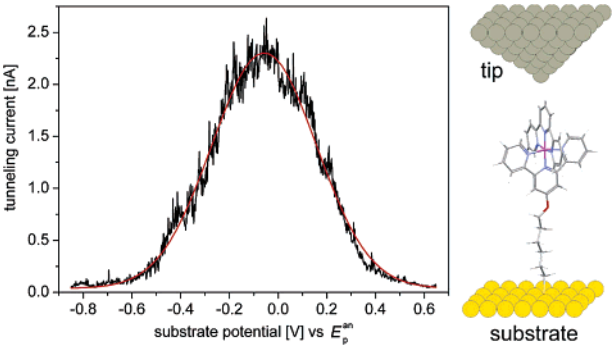


***Figure 2.*** Left: Tunneling current enhancement in $I_t(E_s)_{bias}$ spectroscopy; $V_{bias} = +0.7$ V; sweep duration = 8 s; $I_{set}{}^0 = 0.05$ nA (8 curves averaged); constant tunneling distance; forward (anodic) potential sweep; red line, Gaussian. Right: Tunneling configuration (schematic).

the Fermi window between tip and substrate and induce a strong tunneling current increase. The prominent role of these levels emerges by considering the density of states (DOS) distribution of oxidized and reduced states on the surface, $D_{ox}$ and $D_{red}$, and the individual ET rate constants $k_1$ and $k_2$ (e.g., substrate/molecule, molecule/tip). The products $D_{ox} \times D_{red}$ and $k_1 \times k_2$ and thus the tunneling current $I_t(D_{ox},D_{red},k_1,k_2)$ are maximum at $E^0_{surf}$.

In Figure 3, the bias sweep begins in positive direction at $V_{bias} = -0.7$ V ($E_s = -0.3$ V vs $E_s{}^{an}$(CV), $I_{set}{}^0 = 1.5$ nA). As expected, $I_t$ first decreases with decreasing absolute bias. For $V_{bias} > 0$ V, $I_t$ increases quite rapidly when $E_t$ exceeds the potential of the anodic peak $E_s{}^{an}$ (in CV). Under the conditions used, this refers to the equilibrium peak position after ion pairing. This becomes obvious in the reverse sweep direction (for $V_{bias} = +0.7 \rightarrow -0.7$ V) when

[†] Technical University of Denmark.
[‡] University of Copenhagen.
[§] Risø National Laboratory.


10.1021/ja061993p CCC: $33.50 

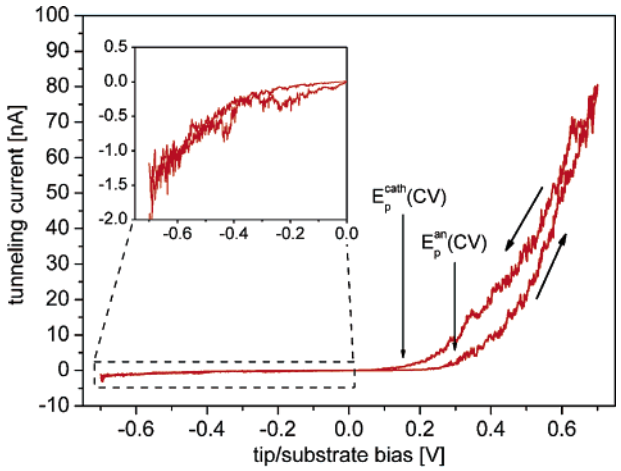


***Figure 3.*** Tunneling current/bias spectroscopy of Ossac at constant $E_s$ in BMI; $E_{s,i} = -0.3$ V; $E_{t,i} = -1.0$ V ($V_{bias,i} = -0.7$ V); forward and reverse sweep indicated; all potentials versus $E_p^{av}$(CV), the average peak position in CV (cf. Figure 2). Positions of anodic and cathodic CV signals on this scale are specified. Inset: Enlarged representation of $I_t$ data for $V_{bias} < 0$ V.

$E_t$ drops below the potential of the cathodic signal in the CV. Ion pairing also explains the apparent hysteresis in Figure 3.

Most importantly, the tip/substrate distance has not changed significantly during the measurement, as the tunneling current at $V_{bias} = -0.7$ V is the same before and after the sweep. The rectification ratio RR generally depends on the potential difference between $E_{s,i}$ and $E^0$ (or $E_p^{an/cath}$). In the present case, RR is large, ~60 for $V_{bias} = \pm 0.7$ V.

The bias range used is already somewhat larger than the accessible potential range in aqueous electrolytes (~1−1.2 V), which is limited by hydrogen and oxygen evolution at low and high potentials, respectively. This highlights a particular advantage of ionic liquids as electrolyte, as their intrinsic stability range can be as large as 6 V.[12] In the present case, however, the electrochemical window is limited by the Au/thiol linker (thiol oxidation/reductive desorption). Ionic liquids further offer high intrinsic (ionic) conductivity, thus minimizing resistance, and extremely low vapor pressure.[12,13] Single-molecule conductivity studies exploiting the increased temperature range, which is essentially limited by melting point and thermal decomposition (about 289 K and 473 K for BMI),[14] would yield important information on details of the charge transfer process.[15]

Their application in single-molecule conductivity studies opens new perspectives toward both fundamental research and application in molecular electronics. In the latter context, they may constitute a step toward true solid-state molecular electronic devices, operated at room temperature and not under cryogenic conditions as previously reported single-molecule devices.[16,17] Transition metal complexes, such as Ossac, or redox-active molecules, in general, add another prospect. As shown, they can be brought to operate both as transistors and diodes with high current modulation by using electrochemical gating. In this way, future electrochemically gated molecular electronic circuitry could be based on a single gate electrode for a whole chip as long as the gate medium is in physical contact with the individual electrodes.

**Methods.** $I_t(E_s)$ spectroscopy was performed by bringing the STM tip (Pt/Ir, 80:20) into tunneling range over a monolayer of Ossac on Au(111) to a predefined setpoint current $I_{set}^0$ at given $V_{bias}$. The initial substrate potential $E_{s,i}$ was set far from the redox potential of the complex, the feedback then switched off, and the substrate potential cycled once in a given potential window at constant $V_{bias}$ and tip/substrate distance. $I_t(V_{bias})$ spectroscopy was performed by keeping the substrate potential $E_s$ constant and only sweeping the tip potential $E_t$ in a predefined potential range. All STM experiments were performed under argon protection and at room temperature (295 K).

**Acknowledgment.** Financial support from the Danish Research Council for Technology and Production Sciences, Nano-Science Center of Copenhagen University, EU IHP training network SUSANA, and Marie Curie fellowship (T.A.) is acknowledged. T.A. would like to thank Solvent Innovation GmbH, Cologne/Germany, for support. The NMR service at OCI, University of Zuerich, is acknowledged for recording the NMR spectra.

**Supporting Information Available:** Electrode and monolayer preparation; details on the synthesis and characterization of Ossac. This material is available free of charge via the Internet at http://pubs.acs.org.

## References

(1) Tao, N. J. *Phys. Rev. Lett.* **1996**, *76*, 4066−4069.
(2) Haiss, W.; van Zalinge, H.; Higgins, S. J.; Bethell, D.; Höbenreich, H.; Schiffrin, D. J.; Nichols, R. J. *J. Am. Chem. Soc.* **2003**, *125*, 15294−15295.
(3) Albrecht, T.; Guckian, A.; Ulstrup, J.; Vos, J. G. *Nano Lett.* **2005**, *5*, 1451−1455.
(4) Albrecht, T.; Moth-Poulsen, K.; Christensen, J. B.; Guckian, A.; Bjørnholm, T.; Vos, J. G.; Ulstrup, J. *Faraday Discuss.* **2006**, *131*, 265−279.
(5) Chen, F.; He, J.; Nuckolls, C.; Roberts, T.; Klare, J. E.; Lindsay, S. *Nano Lett.* **2005**, *5*, 503−506.
(6) Xiao, X.; Nagahara, L. A.; Rawlett, A. M.; Tao, N. J. *J. Am. Chem. Soc.* **2005**, *127*, 9235−9240.
(7) Tran, E.; Rampi, M. A.; Whitesides, G. M. *Angew. Chem., Int. Ed.* **2004**, *43*, 3835−3839.
(8) Alessandrini, A.; Salerno, M.; Frabboni, S.; Facci, P. *Appl. Phys. Lett.* **2005**, *86*, 133902.
(9) Forster, R. J.; Faulkner, L. R. *J. Am. Chem. Soc.* **1994**, *116*, 5444−5452.
(10) Zhang, J.; Chi, Q.; Kuznetsov, A. M.; Hansen, A. G.; Wackerbarth, H.; Christensen, H. E. M.; Andersen, J. E. T.; Ulstrup, J. *J. Phys. Chem. B* **2002**, *106*, 1131−1152.
(11) Kuznetsov, A. M.; Ulstrup, J. *J. Chem. Phys.* **2002**, *116*, 2149−2164.
(12) Buzzeo, M. C.; Evans, R. G.; Compton, R. G. *ChemPhysChem* **2004**, *5*, 1106−1120.
(13) Earle, M. J.; Esperanca, J. M. S. S.; Gilea, M. A.; Canongia Lopes, J. N.; Rebelo, L. P. N.; Magee, J. W.; Seddon, K. R.; Widegren, J. A. *Nature* **2006**, *439*, 831−834.
(14) Kosmulski, M.; Gustafsson, J.; Rosenholm, J. B. *Thermochim. Acta* **2004**, *412*, 47−53.
(15) Haiss, W.; van Zalinge, H.; Bethell, D.; Ulstrup, J.; Schiffrin, D. J.; Nichols, R. J. *Faraday Discuss.* **2006**, *131*, 253−264.
(16) Park, J.; Pasupathy, A. N.; Goldsmith, J. I.; Chang, C.; Yaish, Y.; Petta, J. R.; Rinkoski, M.; Sethna, J. P.; Abruna, H. D.; McEuen, P. L.; Ralph, D. C. *Nature* **2002**, *417*, 722−725.
(17) Kubatkin, S.; Danilov, A.; Hjort, M.; Cornil, J.; Brédas, J.-L.; Stuhr-Hansen, N.; Hedegard, P.; Bjørnholm, T. *Nature* **2003**, *425*, 698−701.

JA061993P